

Mechanical Design and Modeling of an Omni-directional RoboCup Player

Brian Carter¹, Matt Good¹, Mike Dorohoff¹, Jae Lew¹, Robert L. Williams II¹, Paolo Gallina²

¹Department of Mechanical Engineering
Ohio University, USA

²Department of Innovation in Mechanics and Management
University of Padova, Italy

Abstract. This paper covers the mechanical design process of an omni-directional mobile robot developed for the Ohio University RoboCup team player. It covers each design iteration, detailing what we learned from each phase. In addition, the kinematics of the final design is derived, and its inverse Jacobian matrix for the design is presented. The dynamic equations of motion for the final design is derived in a symbolic form, assuming that no slip occurs on the wheel in the spin direction. Finally, a simulation example demonstrates simple independent PID wheel control for the complex coupled nonlinear dynamic system.

1 Introduction

Research interest in mobile robots has been tremendous in the past few years, as evidenced by review articles (e.g. [1,2]). The RoboCup 2000 competition in Sydney, Australia proved that omni-directional mobile robot platforms are desirable for agility. Many research groups are studying omni-directional mobile robots and vehicles [3-7].

This project began when a cross-disciplinary group of Ohio University engineering students and faculty (Electrical Engineering, Computer Science, and Mechanical Engineering) decided to take part in the 2001 RoboCup Competition. The Ohio University RoboCup team consists of 4 players and 1 goalie. They have separate mechanical/electrical/software designs to meet different performance requirements as a player and a goalie. For example, the players are designed to optimize forward motion with omni-directional capability, while the goalie is designed to optimize side-to-side motion with omni-directional capability equipped with a local vision camera. This paper will detail the mechanical design process of the player, the kinematics and dynamics of the final design, and simulation results.

2 Design

There were several factors that influenced the design of the Ohio University RoboCup 2001 player robot. It was necessary for the robot to be agile, but heavy enough not to be pushed around by other teams on the field. The robot should also be able to "kick" the ball relatively hard, with a degree of accuracy.

2.1 The Phase II Robot

The mechanical engineering design process began with what was known as the Phase II RoboCup Robot (see Figure 1). Designed by a former Ohio University graduate student, this was a simple two wheeled robot with skids on the front and a roller ball on the back. The kicking mechanism consisted of a solenoid propelling an aluminum block forward, "kicking" the ball. However, in practice, this design had several faults. The four supports didn't provide the necessary stiffness, and the kicking mechanism never worked properly.

The final flaw in the Phase II RoboCup Robot design became apparent from a videotape of the RoboCup 2000 competition. Many of the robots on this tape possessed two greatly desired capabilities: omni-directional locomotion, and a "dribble-bar". Omni-directional locomotion is the ability to move in any direction while facing any orientation. The "dribble-bar" is a spinning rod on the front of the robot allowing the robot to impart backspin on the ball. This backspin allows the robot to maintain control of the ball while moving.

Several different methods of omni-directional locomotion were considered, but most were too bulky, or the wheels were too expensive. However, one relatively simple solution fit our size constraints, as well as our budget. Three wheels, which were able to have free rotation in one direction, and powered rotation in an orthogonal direction, should enable omni-directional movement [6].

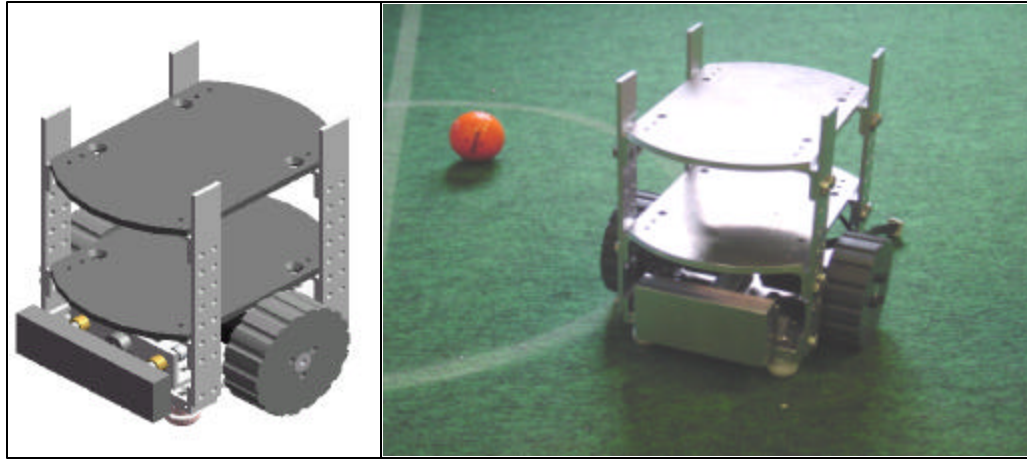


Fig. 1. The Phase II RoboCup Robot.

2.2 The Phase III RoboCup Robot

The next design iteration undertaken was dubbed the Phase III, and followed the theory of [6] exactly, making the dynamics of this Phase the simplest of any alternative considered due to the inherent symmetry of the design. The wheels were arranged in a symmetrical manner, 120° apart. As can be seen from Figure 2, this Phase only made it as far as the basic design, as there was no way to fit in a kicking mechanism of suitable size while maintaining observance to the RoboCup rules. However, it was used as a test bed to verify that the selected motors would be able to move the vehicle at a sufficient velocity for the competition. Special note should be taken of the wheels, shown in Figure 3.

These wheels, produced by the Kornylak corporation [9] and dubbed the Transwheel, were designed for the material processing industry. Not only are they sturdy (up to 25 lb), they're also economical (\$2.50/wheel). As can be seen from Figure 3, the wheels can be used for powered rotation along the primary diameter, just as any other wheel. However, the smaller rollers along the outside of this diameter allow free rotation along an orthogonal direction to the powered rotation.

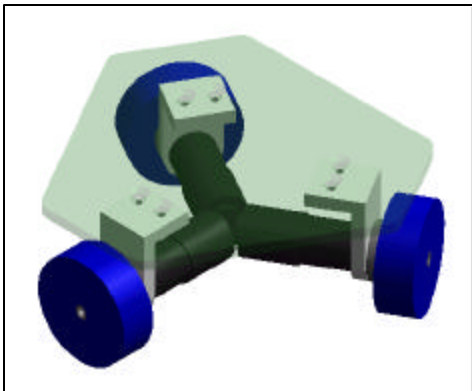


Fig. 2. The Phase III RoboCup Robot



Fig. 3. The Transwheel™, used on the Ohio University player

Due to the size limitations from the RoboCup rules, the Phase III had to be compromised. To make room for a kicking apparatus, the symmetry of the Phase III would have to be lost, complicating the kinematics and dynamics calculations. However, this change in geometry did optimize the speed in the forward direction, with a corresponding loss of overall omni-directional agility.

2.3 The Phase IIIB RoboCup Robot

The next design was dubbed the Phase IIIB, and displays the kicker/dribbler design created by Mechanical Engineering undergraduate students working on this project. As can be seen from Figure 4, the bar at the

front of the robot is the dribble bar. The bar that rotates about the dribbler is the kicker bar. Unlike the Phase III, the Phase IIIB's front wheels are at a 105° angle from the back wheel, rather than the symmetrical 120° . However, this allowed a full 5" of kicker area, allowing easier contact with the ball. This was the sturdiest design, and was promising.

Unfortunately, there were some design issues that the prototype of the Phase IIIB brought up. The first was the height restriction. With this design, we had approximately 3.5" of available space for the electrical components necessary to run the robot. Since we wanted to maximize the amount of payload, several design suggestions were implemented in the next design iteration.

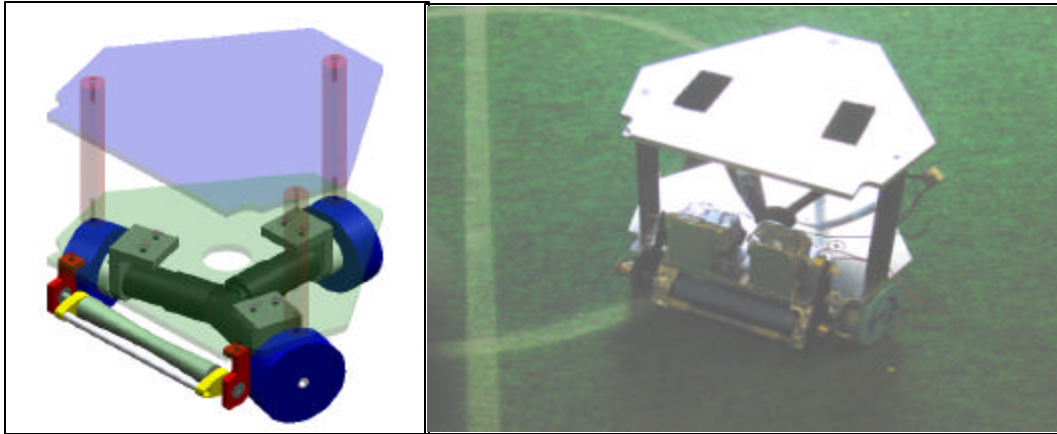


Fig. 4. The Phase IIIB RoboCup Robot.

2.4 The Phase IV RoboCup Robot

The final design, dubbed the Phase IV (see Figure 5), was the final product of the previous designs. Although it is very similar to the Phase IIIB, it has recessed wheels (i.e., notches cut into the base plate allowing the chassis to sit lower on the wheels, much like the wheel wells of a car), as well as a thinner top plate and motor mounts. This increased the vertical space within the robot by just over half an inch, allowing more room for the required circuits and processors.

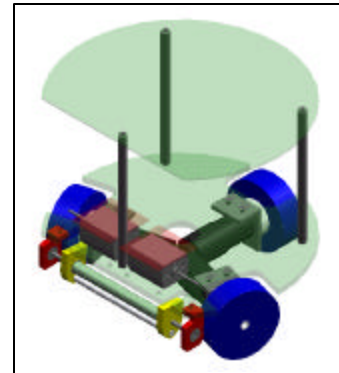


Fig. 5. The Phase IV RoboCup Robot.

3 Kinematics of the Phase IV RoboCup Robot

The inverse kinematic model for the Phase IV was relatively simple to devise. As can be seen from Figure 6, the moving frame $[x_m, y_m]^T$ is located at the center of gravity of the robot. The two front wheels (1 and 2) are offset from y_m by fixed angle \mathbf{d} . Please note that the arrows projecting from each of the three wheels indicates the velocity vector generated by that wheel when rotating in the positive direction.

The inverse Jacobian matrix was relatively simple to calculate. As can be seen in Figure 6, the velocity vectors generated by each wheel (labeled 1, 2, and 3) are offset from the y_w axis by three angles. These angles are: $(\mathbf{d} + \mathbf{f})$ for 1, $(\mathbf{d} - \mathbf{f})$ for 2, and $(90 - \mathbf{f})$ for 3. Given that the velocity vector for wheel i is given as $R\mathbf{q}_i$, it is simple to compute the necessary wheel speed for a desired Cartesian velocity, as can be seen in equations (1)-(3).

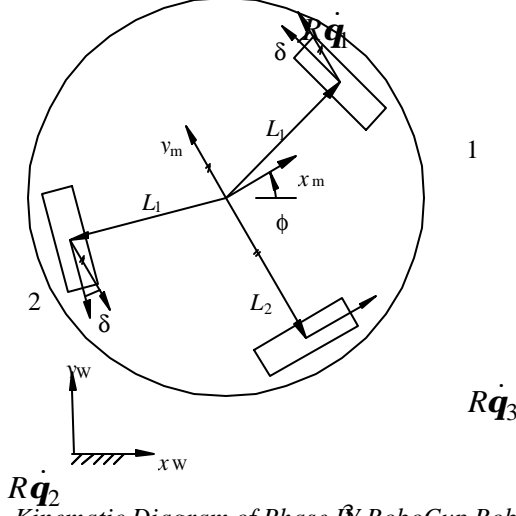


Fig. 6. Kinematic Diagram of Phase I RoboCup Robot.

The inverse kinematic equations are as follows:

$$R\dot{\mathbf{q}}_1 = -\sin(\mathbf{d} + \mathbf{f})\dot{x}_w + \cos(\mathbf{d} + \mathbf{f})\dot{y}_w + L_1\dot{\mathbf{f}} \quad (1)$$

$$R\dot{\mathbf{q}}_2 = -\sin(\mathbf{d} - \mathbf{f})\dot{x}_w - \cos(\mathbf{d} - \mathbf{f})\dot{y}_w + L_1\dot{\mathbf{f}} \quad (2)$$

$$R\dot{\mathbf{q}}_3 = \cos(\mathbf{f})\dot{x}_w + \sin(\mathbf{f})\dot{y}_w + L_2\dot{\mathbf{f}} \quad (3)$$

Please note that the constant L_1 refers to the distance from the center of gravity of the robot to the center of the two front wheels (1 and 2) along a radial path. The constant L_2 refers to the distance from the center of gravity of the robot to the center of the rear wheel (3) along a radial path. $[x_w, y_w]$ is the fixed world frame, \mathbf{f} is the orientation of the robot with respect to the fixed world frame, R is the radius of the wheels, and \mathbf{q} is the angular position of each wheel. The constant δ refers to the wheel orientation with respect to the mobile robot frame. For the Ohio University design, this value is 15° . Equations (1)-(3) allow us to form the inverse Jacobian matrix for the system, as follows:

$$\begin{Bmatrix} \dot{\mathbf{q}}_1 \\ \dot{\mathbf{q}}_2 \\ \dot{\mathbf{q}}_3 \end{Bmatrix} = \frac{1}{R} \begin{bmatrix} -\sin(\mathbf{d} + \mathbf{f}) & \cos(\mathbf{d} + \mathbf{f}) & L_1 \\ -\sin(\mathbf{d} - \mathbf{f}) & -\cos(\mathbf{d} - \mathbf{f}) & L_1 \\ \cos(\mathbf{f}) & \sin(\mathbf{f}) & L_2 \end{bmatrix} \begin{Bmatrix} \dot{x}_w \\ \dot{y}_w \\ \dot{\mathbf{f}} \end{Bmatrix} \quad (4)$$

4 Dynamics

A dynamic model for the robot was difficult to derive. Although there was an existing derivation for a similar model [6], the lack of symmetry in the Ohio University wheel design caused complications. The derivation began with Newton's Second Law:

$$M\ddot{x}_w = F_x$$

$$M\ddot{y}_w = F_y \quad (5),(6),(7)$$

$$I_v\ddot{\mathbf{f}} = M_l$$

where M is the mass of the mobile robot, I_v is the moment of inertia of the mobile robot, F_x and F_y are the Cartesian forces acting upon the robot with respect to the world frame, and M_l is the moment acting upon the center of gravity of the mobile robot.

Please note that the Cartesian dynamics equations (5) and (6) are given with respect to the world frame and need to be transformed to the moving frame to aid the derivations. After transformation, the following equations are revealed.

$$M(\ddot{x}_m - \dot{y}_m \dot{\mathbf{f}}) = f_x \quad (8), (9)$$

$$M(\ddot{y}_m + \dot{x}_m \dot{\mathbf{f}}) = f_y$$

Please note that f_x and f_y refer to the Cartesian forces acting upon the mobile robot with respect to the world frame in terms of the mobile robot frame, and x_m and y_m refer to the Cartesian position with respect to the world frame in terms of the mobile robot frame. f_x, f_y , and M_I are given by:

$$f_x = -\sin(\mathbf{d})D_1 - \sin(\mathbf{d})D_2 + D_3 \quad (10), (11), (12)$$

$$f_y = \cos(\mathbf{d})D_1 - \cos(\mathbf{d})D_2$$

$$M_I = (D_1 + D_2)L_1 + D_3L_2$$

where D_i is the driving force due to each wheel assembly.

The driving system dynamic model for each wheel is assumed to be given by [10]:

$$I_w \ddot{\mathbf{q}}_i + c \dot{\mathbf{q}}_i = k u_i - R D_i \quad (13)$$

for $i = 1, 2, 3$. I_w is the moment of inertia of the wheel assemblies, \mathbf{q} is the angular position of each wheel, c is the viscous friction factor of the wheel assembly, k is the driving gain factor, u_i is the driving input torque, and R is the radius of the wheels.

The inverse kinematic equations for the mobile robot with respect to the mobile robot frame are shown below.

$$\begin{Bmatrix} \dot{\mathbf{q}} \\ \dot{\mathbf{q}} \\ \dot{\mathbf{q}} \end{Bmatrix} = \frac{1}{R} \begin{bmatrix} -\sin(\mathbf{d}) & -\cos(\mathbf{d}) & L_1 \\ -\sin(\mathbf{d}) & \cos(\mathbf{d}) & L_1 \\ 1 & 0 & L_2 \end{bmatrix} \begin{Bmatrix} \dot{x}_m \\ \dot{y}_m \\ \dot{\mathbf{f}} \end{Bmatrix} \quad (14)$$

Using equation (14) and its derivatives, and plugging this into equation (13) and solving for D_i calculates the driving force due to each wheel. Substituting these values into equations (10)-(12), and substituting these into equations (7)-(9) allows the equations of motion to be represented in the standard format.

$$[P]\{\ddot{X}_m\} + \{N(X_m, \dot{X}_m)\} = [A]\{U\} \quad (15)$$

where:

$$P = \begin{bmatrix} \frac{MR^2 + 2I_w \sin^2(\mathbf{d}) + I_w}{MR^2} & 0 & \frac{-2I_w \sin(\mathbf{d})L_1 + I_w L_2}{MR^2} \\ 0 & \frac{MR^2 + 2I_w \cos^2(\mathbf{d})}{MR^2} & 0 \\ \frac{-2L_1 I_w \sin(\mathbf{d}) + L_2 I_w}{I_w R^2} & 0 & \frac{I_w R^2 + I_w L_2^2 + 2I_w L_1^2}{I_w R^2} \end{bmatrix} \quad (16)$$

$$N = \left\{ \begin{array}{l} \frac{(2c - c \cos(2\mathbf{d}))\dot{x}_m}{MR^2} + \frac{(cL_2 - 2c \sin(\mathbf{d}))L_1 \dot{\mathbf{f}}}{MR^2} - \dot{y}_m \dot{\mathbf{f}} \\ \frac{2c \cos^2(\mathbf{d})\dot{y}_m + \dot{x}_m \dot{\mathbf{f}}}{MR^2} \\ \frac{(-2L_1 c \sin(\mathbf{d}) + L_2 c)\dot{x}_m}{I_w R^2} + \frac{(2cL_1^2 - cL_2^2)\dot{\mathbf{f}}}{I_w R^2} \end{array} \right\} \quad (17)$$

$$A = \begin{bmatrix} \frac{-\sin(\mathbf{d})k}{MR} & \frac{-\sin(\mathbf{d})k}{MR} & \frac{k}{MR} \\ \frac{\cos(\mathbf{d})k}{MR} & \frac{-\cos(\mathbf{d})k}{MR} & 0 \\ \frac{L_1 k}{I_w R} & \frac{L_1 k}{I_w R} & \frac{L_2 k}{I_w R} \end{bmatrix} \quad (18)$$

5 Simulation

Given equations (15)-(18), it was possible to simulate the nonlinear system dynamics using Simulink, the graphical Matlab workspace. The controller used was a wheel independent Proportional-Integral-Derivative controller, as a preliminary study.

The responses of the system to a simple step-input for position, while maintaining a fixed orientation (0°), are shown below. Please note that this simulation deals only with mechanical factors (weight, inertia, etc.) and ignores any electrical components. Also, this model does not account for any slippage occurring. Therefore, the real world behavior may not closely mimic this simulation.

As can be seen from Figure 8, the overshoot is approximately 10% for the XPosition and 5% for the Y Position, and the settling time is approximately 0.08 seconds. As shown in the bottom graph, the orientation fluctuates briefly while the robot moves to the desired position, but quickly returns to the desired value of 1.57 rad (90°).

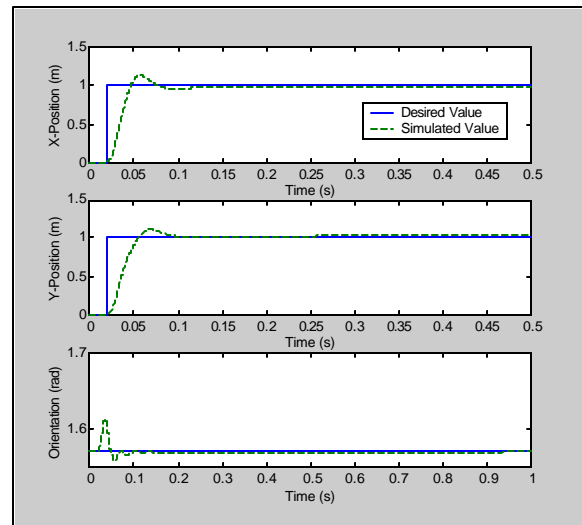


Fig. 7. Response of Simulated Phase IV RoboCup Robot to a Step Input.

6. Conclusion

This paper presents design, modeling, and simulation for the Ohio University 2001 RoboCup player robot. We have developed an omni-directional motion base using omni-directional wheels over several prototype iterations. We have presented the kinematics and dynamics equations, plus preliminary control simulation results using simple independent PID wheel control with the coupled nonlinear dynamics model.

References

- [1] C.C. De Wit, 1998, "Trends in Mobile Robot and Vehicle Control", *Control Problems in Robotics and Automation*, 151-175.
- [2] J. Borenstein, H.R. Everett, and L. Feng, 1997, "Mobile Robot Positioning: Sensors and Techniques", *Journal of Robotic Systems*, 14: 231-249.
- [3] S.L. Dickerson and B.D. Lapin, 1991, "Control of an Omni-Directional Robotic Vehicle with Mecanum Wheels", *National Telesystems Conference Proceeding*, 1: 323-328.
- [4] M.-J. Jung, H.-S. Kim, S. Kim, and J.-H. Kim, 2000, "Omni-Directional Mobile Base OK-II", *Proceedings of the IEEE International Conference on Robotics and Automation*, 4: 3449-3454.
- [5] Y. Mori, E. Nakano, T. Takahashi, and K. Takayama, 1999, "Mechanism and Running Modes of New Omni-Directional Vehicle ODV9", *JSME International Journal, Series C*, 42(1): 210-217.
- [6] K. Watanabe, Y. Shiraishi, S. Tzafestas, J. Tang, and T. Fukuda, 1998, "Feedback Control of an Omni-directional Autonomous Platform for Mobile Service Robots", *Journal of Intelligent and Robotic Systems*, 22: 315-330.
- [7] G. Witus, 2000, "Mobility Potential of a Robotic 6-Wheeled Omni-Directional Drive Vehicle (ODV) with Z-Axis and Tire Inflation Control", *Proceedings of SPIE*, 4024: 106-114.
- [8] <http://arti.vub.ac.be/RoboCup/rules/rules.html> RoboCup 2001 Rules Draft Site.
- [9] <http://kornylak.com/> Website for the Kornylak Corporation
- [10] Saito, M., Tsumura, T. "Collision Avoidance Among Multiple Mobile Robots - A Local Approach Based on Nonlinear Programming", *Trans. of the Institute of Systems, Control and Information Engineers*, 3(8) (1990) 252-260.